Turkish Journal of Chemistry

http://journals.tubitak.gov.tr/chem/

Research Article

Turk J Chem
(2014) 38: 28 – 40

doi:10.3906/kim-1301-87

Immobilized metal ion affinity nanospheres for α-amylase immobilization

Tülden KALBURCU[1], Münire Nalan TÜZMEN[2,*], Sinan AKGÖL[3], Adil DENİZLİ[4]

[1]Department of Chemistry, Faculty of Science and Arts, Aksaray University, Aksaray, Turkey
[2]Department of Chemistry, Faculty of Science, Dokuz Eylül University, İzmir, Turkey
[3]Department of Biochemistry, Faculty of Science, Ege University, İzmir, Turkey
[4]Department of Chemistry, Faculty of Science, Hacettepe University, Ankara, Turkey

Received: 31.01.2013 • **Accepted:** 25.04.2013 • **Published Online:** 16.12.2013 • **Printed:** 20.01.2014

Abstract: Immobilized metal chelate affinity chromatography (IMAC) support was practiced for α-amylase immobilization. Poly(hydroxyethylmethacrylate-methacryloylamidotryptophan)-Ni^{2+} [p(HEMA-MAT)-Ni^{2+}] nanospheres, average diameter 100 nm, were produced by surfactant free emulsion polymerization. Characterizations of p(HEMA-MAT)-Ni^{2+} nanospheres were carried out by Fourier transform infrared (FTIR) spectroscopy and scanning electron microscope (SEM). In addition, average particle size, size distribution, and surface charge were specified. The amount of N-methacryloylamidotryptophan (MAT) incorporated to polymer was determined as 1.95 mmol/g polymers by using nitrogen stoichiometry. The specific surface areas of poly(hydroxyethylmethacrylate) [p(HEMA)] and p(HEMA-MAT) nanospheres were calculated as 1856 m^2/g and 1914 m^2/g, respectively. Protein adsorption increased with increasing initial protein concentration and maximum α-amylase adsorption on p(HEMA-MAT)-Ni^{2+} nanospheres was observed at pH 4.0. Both free and immobilized α-amylase showed pH optimum at pH 7.0. It was determined that the immobilized α-amylase had better thermostability than the free one. Immobilization of the enzyme did not significantly change the kinetic parameters. The storage stability of α-amylase increased upon immobilization. It was also observed that p(HEMA-MAT)-Ni^{2+} nanospheres can be repeatedly used for α-amylase immobilization.

Key words: α-Amylase, nanospheres, IMAC, enzyme immobilization, adsorption

1. Introduction

One of the hydrolyzing enzymes widely used in different industries is α-amylase (1,4-α-d-glucan-glucanhydrolase, EC. 3.2.1.1), which is an endo-acting enzyme. While α-amylase hydrolyzes the α-1,4-glycosidic bonds, it bypasses α-1,6-glycosidic linkages in starch and related substrates.[1−4] Starch hydrolysis by α-amylase to low molecular weight products is widely utilized in the food, paper, textile, distillery, and brewing industries.[5] Amylase cannot be used repeatedly because of its poor stability.[6,7] Amylase immobilization on water insoluble carriers appears to be the most hopeful way to get more stable products for multiple uses.[8−15] Enzyme immobilization can be achieved by several methods. These immobilization methods consist of enveloping the enzyme into a gel matrix, encapsulation, incorporation into emulsions and membranes, binding to a support by adsorption, coordination, or covalent binding. Among these immobilization methods, adsorption has the advantages of improving the control of the reactor, permitting reuse of the enzyme, and avoiding protein contamination of the final product. In other respects, noncovalent adsorption techniques may be a good option

*Correspondence: nalan.tuzmen@deu.edu.tr

due to being simple and requiring little work and time. Otherwise, inactivated enzyme can be desorbed and supports can be used again. This decreases the final price and amounts of residues.[16] In the past few decades, many immobilization methods and carrier materials have been investigated.[17,18] Inorganic supports, synthetic polymers, and natural macromolecules are classified as carrier materials for enzyme immobilization.[19] Polymeric carriers have the advantageous of good mechanical properties, ease of preparation, and applicability to introduce bio-friendly components for improving biocompatibility. Additionally, reactive functional groups on polymeric carriers provide necessary interactions with the enzymes.[20,21] Many studies about synthesis of micro-sized polymeric matrices and their applicability in protein separation with the succor of a specific ligand coating the surface of the particles are published.[22] Unfortunately, studies on the application of nanosized particles in the immobilization of enzymes are very limited. Nanoparticles can produce larger specific surface area due to their nanoscopic size and hence higher protein binding capacity may be determined. Consequently, nanosized particles with large surface areas may be suitable carriers for enzyme immobilization.[23,24] While immobilizing an enzyme into porous materials, a decrease in mass-transfer resistance is assumed for smaller porous particles. The reason for this expectation is the shortened diffusional path of substrates when compared to large-sized porous materials. As a result, nanoparticles provide several advantages in the optimization of immobilized enzymes: minimum diffusional limitation, maximum surface area per unit mass, and high enzyme loading.[25]

Immobilized metal-affinity chromatography (IMAC), introduced by Porath et al. in 1975,[26] has become a prevalent analytical and preparative separation method. This separation method can be used for therapeutic proteins, peptides, nucleic acids, hormones, and enzymes.[27] Covalently bound chelating compounds on solid chromatographic supports are used in IMAC to entrap metal ions. These metal ions used as affinity ligands generate coordinative binding with some amino acid residues exposed on protein surfaces.[28] IMAC is more favorable than other biospecific affinity chromatographic techniques that have a similar order of affinity constants. The benefits of IMAC can be compiled as ligand stability, high protein loading, rapid purification, mild elution conditions, simple regeneration, and low cost. In industrial applications, these benefits are critical when developing large-scale purification procedures.[29]

In the present study, poly(hydroxyethylmethacrylate-methacryloylamidotryptophan) p(HEMA-MAT) nanospheres were synthesized by surfactant free emulsion polymerization of 2-hydroxyethyl methacrylate (HEMA) and MAT. Then p(HEMA-MAT) nanospheres were incorporated with Ni^{2+} ions. This newly coined IMAC support was characterized by FTIR spectroscopy, SEM, elemental analysis, particle size, and surface area measurements and then used in α-amylase immobilization. α-Amylase adsorption onto these metal-chelated nanospheres was optimized by varying different parameters such as pH, initial α-amylase concentration, temperature, and ionic strength. Desorption of α-amylase and reusability of these metal-chelated affinity nanospheres and the kinetic parameters of the enzyme (K_M and V_{max}) were also tested.

2. Results and discussion

2.1. Characterization of p(HEMA-MAT)-Ni^{2+} nanospheres

This study has the characteristic advantage of the elimination of the activation and ligand coupling steps during the preparation of the affinity matrices. Moreover, using a known amount of ligand in the polymer preparation mixture and the good reproducibility of the affinity matrix are further advantages over other methods.

FTIR spectra of p(HEMA), p(HEMA-MAT), and p(HEMA-MAT)-Ni^{2+} nanospheres are shown in Figure 1. Stretching vibration of hydroxyl groups of both p(HEMA), p(HEMA-MAT), and p(HEMA-MAT)-Ni^{2+}

nanospheres was observed at around 3500 cm^{-1}. The peaks at this wavenumber of p(HEMA-MAT) and p(HEMA-MAT)-Ni^{2+} nanospheres are sharper than the peak of the p(HEMA) because of the extra stretching vibration of the hydroxyl group of MAT in the p(HEMA-MAT) and p(HEMA-MAT)-Ni^{2+} nanospheres. The change in the FTIR spectrum of p(HEMA-MAT) and p(HEMA-MAT)-Ni^{2+} nanospheres around 3000–3400 cm^{-1} also depends on the existence of N–H stretching and aromatic C–H stretching bands of L-tryptophan. As known, the Ni^{2+} ion incorporates with the nitrogen atom of the indole ring and the oxygen atom of the hydroxyl group of carboxylic acid in tryptophan. Due to metal incorporation, electron density of these groups moves towards the metal ion. Therefore, a shift in the frequencies of the N–H stretching band from 3378 nm to 3375 nm was observed with Ni^{2+} incorporation.

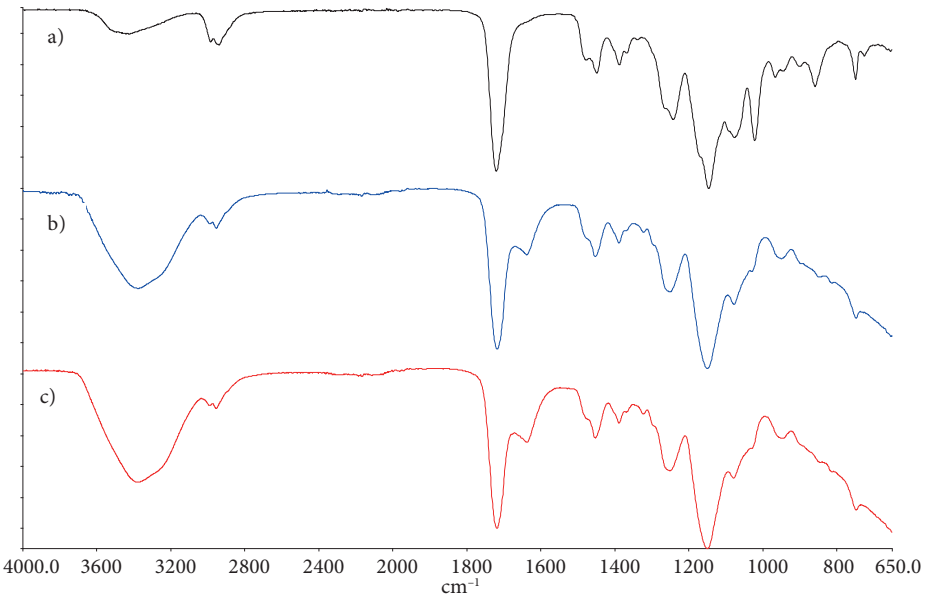

Figure 1. FTIR spectra of the p(HEMA) (a), p(HEMA-MAT) (b), and p(HEMA-MAT)-Ni^{2+} nanospheres.

In the FTIR spectrum of p(HEMA-MAT) and p(HEMA-MAT)-Ni^{2+} nanospheres, the peak at 1638 cm^{-1} confirmed the formation of an amide bond between HEMA and MAT. The band obtained at 1045 cm^{-1} in the FTIR spectrum of p(HEMA-MAT) and p(HEMA-MAT)-Ni^{2+} nanospheres was assigned to the in-plane deformation of C-H (βCH) in the indole ring of tryptophan. The C–O stretching band that appeared at 1322 cm^{-1} came from the carboxylic acid group of tryptophan in the structure of p(HEMA-MAT) and p(HEMA-MAT)-Ni^{2+} nanospheres. The peak in this wavenumber of p(HEMA-MAT)-Ni^{2+} nanospheres is sharper than the peak of the p(HEMA-MAT) because of the chelate formation with metal ion. The strength of the O–H bending band of the carboxylic acid group of tryptophan observed at around 950 cm^{-1} also changed in the FTIR spectrum of p(HEMA-MAT)-Ni^{2+} nanospheres through chelation (Figure 1). These data confirmed the existence of MAT and Ni^{2+} ions in the structures of p(HEMA-MAT) and p(HEMA-MAT)-Ni^{2+} nanospheres.

The particle size of the p(HEMA-MAT)-Ni^{2+} nanospheres was measured by Zeta Sizer at about 100 nm with 1.189 polydispersity (Figure 2).

At least 30 measurements were carried out to specify the particle sizes and the software recorded the size distributions automatically. The degree of MAT incorporation into the polymeric structure was determined via

elemental analysis of the synthesized p(HEMA-MAT) nanospheres. The MAT incorporation was determined as 1.95 mmol/g polymer by using nitrogen stoichiometry. The specific surface areas of p(HEMA) and p(HEMA-MAT) nanospheres were calculated as 1856 and 1914 m^2/g, respectively. A SEM photograph of p(HEMA-MAT) nanospheres is shown in Figure 3 and indicates their spherical character.

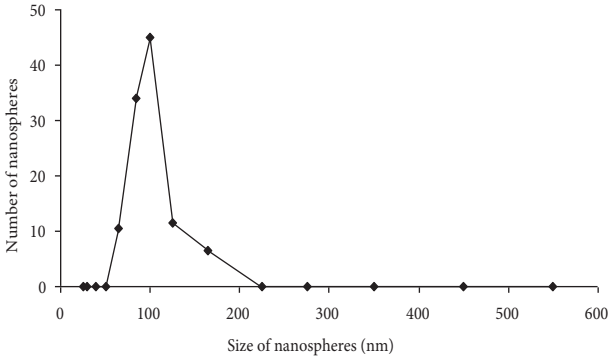

Figure 2. Particle size of the p(HEMA-MAT) nanospheres.

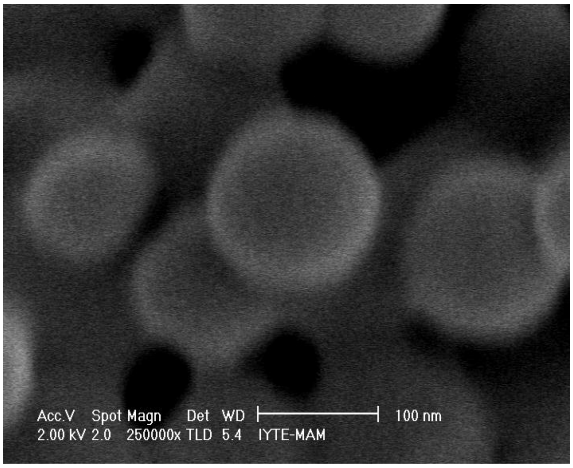

Figure 3. Scanning electron micrograph of the p(HEMA-MAT) nanospheres.

2.2. Effect of pH on α-amylase adsorption

Maximum α-amylase adsorption was determined at pH 4.0 and the amount of α-amylase adsorbed onto the p(HEMA-MAT)-Ni^{2+} nanospheres showed a significant decrease at lower and higher pH values (Figure 4). Different parameters affecting the protein retention on immobilized metal ion affinity matrices can be listed as follows:

1. Electrostatic (or ionic) interaction may take place between the charged biomolecules and positively charged metal ions and the negatively charged sites remaining on the matrix surface (such as the unreacted functional groups from the basic membrane materials, or the residual carboxyl groups for dentate chelators) due to the incomplete chelator coupling of metal ion immobilization.

2. Hydrophobic interactions may occur between biomolecules and the hydrophobic sites on the matrix surface.

3. Donor–acceptor (coordination) interactions may happen between the exposed amino acid residues (such as the imidazole groups of the histidine residues) on the biomolecule surface and the immobilized metal ions.[30]

Therefore, the ionization states of several groups on both the matrices (i.e. carboxylic acid and amino groups and Ni^{2+} ions) and amino acid side chains in α-amylase, and the conformational state of α-amylase molecules (more folded structure) at this pH may be the reason for the specific interactions (hydrophobic, electrostatic, and hydrogen bonding) between α-amylase and the p(HEMA-MAT)-Ni^{2+} nanospheres at pH 4.0. Moreover, electrostatic repulsions between enzyme and Ni^{2+} ions on the matrix increase because of the cationic surface of the enzyme at alkaline pH. Thus, a decrease in the adsorption capacity of matrix was determined.

2.3. Effect of the initial concentration on α-amylase adsorption

Effect of the initial concentration of α-amylase on adsorption is shown in Figure 5. It is clearly seen from this figure that the amount of adsorbed α-amylase increased with increasing initial α-amylase concentration. Nonspecific α-amylase adsorption on the plain p(HEMA) nanospheres (33.0 $\pm$ 2.9 mg/g) was negligible. The increase in the adsorption capacity of p(HEMA-MAT)-Ni^{2+} nanospheres can be explained by the ternary complex formation between Ni^{2+} ions, MAT, and protein molecules.

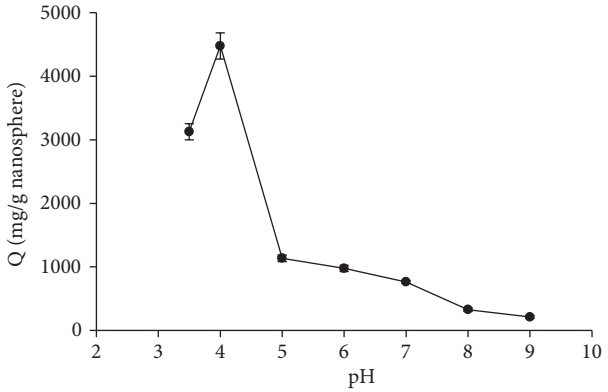

Figure 4. Effect of pH on α-amylase adsorption onto p(HEMA-MAT)-Ni^{2+} nanospheres (c: 1.0 mg/mL, T: 25 °C, time: 60 min).

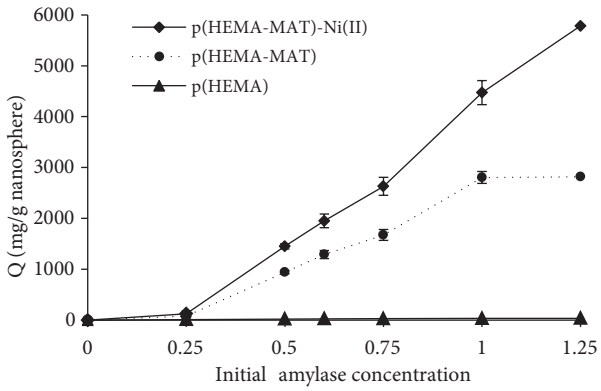

Figure 5. Effect of the initial concentration on α-amylase adsorption onto the p(HEMA), p(HEA-MAT), and p(HEMA-MAT)-Ni^{2+} nanospheres (pH: 4.0; T: 25 °C; time: 60 min).

The amount of α-amylase adsorbed per unit mass of the p(HEMA-MAT) nanospheres increased first with increasing α-amylase concentration and then reached a plateau value at 1 mg/mL. The active adsorption sites on the nanospheres may be saturated with protein molecules at this α-amylase concentration. The maximum amount of α-amylase adsorbed on the p(HEMA-MAT) nanospheres was determined as 2803.4 $\pm$ 107.0 mg/g at this concentration. A nearly 2-fold increase was observed in the adsorption capacity of p(HEMA-MAT)-Ni^{2+} nanospheres (4468.1 $\pm$ 177.5 mg/g) at the same concentration. The electron donating side chains of proteins, such as histidine and cysteine, are connected to metals. The chelate polymer structure and pH influence the binding.[31] The reason for this increase observed in the adsorption capacity of the Ni^{2+}-chelated p(HEMA-MAT) nanospheres may be these high specific interactions.

2.4. Effect of ionic strength on α-amylase adsorption

The α-amylase adsorption capacity of p(HEMA-MAT)-Ni^{2+} nanospheres decreased about 40.0% with increasing NaCl (Figure 6). Protein stability changes in different salt solutions because of the ion-specific effect of salts. Stabilizing or destabilizing effects of salts may be arranged typically following the Hofmeister series:

$$SO_4^{2-} > H_2PO_4^- > CH_3COO^- > Cl^- > Br^- > I^- > ClO_4^- > SCN^-.$$

The physicochemical properties and interactions between proteins are affected by salts such as Na_2SO_4, NaCl, NaBr, NaI, $NaClO_4$, and NaSCN. Additionally, these salts may change water structure by altering the hydrophobic and electrostatic interactions at high concentrations.[32] Binding forces within the matrices of protein molecules, such as hydrophobic and electrostatic interactions, can be influenced by ionic strength and

these changes result in varying structural conformations and functional properties. Adding kosmotropic salts such as NaCl and NaBr to the adsorption medium sustainably affects the protein adsorption on IMAC gels.[30]

Our results indicate that hydrophobic interactions between the attached MAT molecules themselves would become much more dominant. Thus, the adsorption of the α-amylase to the attached MAT molecules became difficult because of the decrease in the numbers of MAT molecules, which interact with α-amylase with increasing ionic strength. It can be also concluded that the reason for the reduction in electrostatic interactions between protein molecules and chelated Ni^{2+} ions on the nanospheres may be an increase in NaCl concentration.

2.5. Effect of temperature on α-amylase adsorption

Effect of temperature on α-amylase adsorption was studied in the range of 5–45 °C. As seen in Figure 7, the α-amylase adsorption capacity of the p(HEMA-MAT)-Ni^{2+} nanospheres significantly increased with increasing temperature. A 54.89% increase in the adsorption capacity of p(HEMA-MAT)-Ni^{2+} nanospheres was determined as temperature was raised from 5 to 45 °C. There are cumulative effects of electrostatic (or ionic), hydrophobic, and/or donor–acceptor (coordination) interactions in the adsorption on IMAC matrices.[33] The increase observed in adsorption capacity may be due to the increase in Van der Waals attraction forces with increasing temperature.

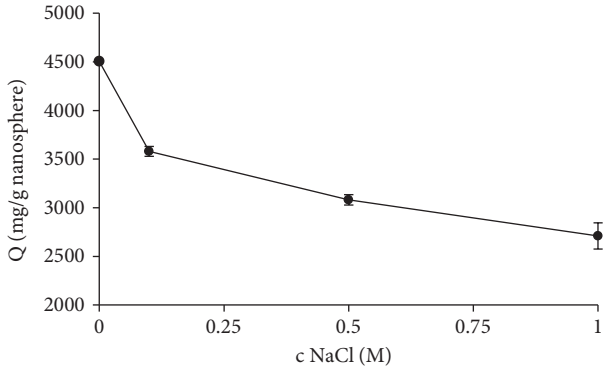

Figure 6. Effect of ionic strength on α-amylase adsorption onto the p(HEMA-MAT)-Ni^{2+} nanospheres (pH: 4.0; c: 1.0 mg/mL; T: 25 °C; time: 60 min).

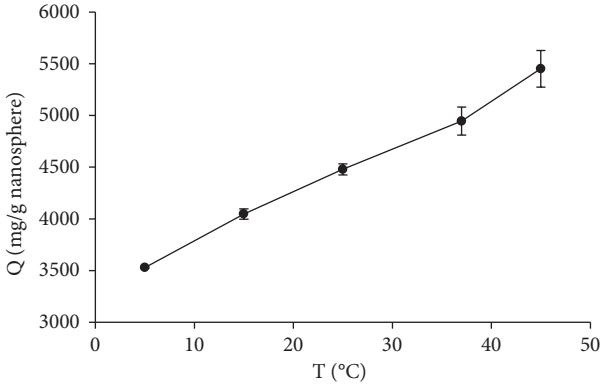

Figure 7. Effect of temperature on α-amylase adsorption onto the p(HEMA-MAT)-Ni^{2+} nanospheres (pH: 4.0; c: 1.0 mg/mL; time: 60 min).

2.6. Desorption and repeated use

Sodium chloride solution (1.5 M) was chosen as desorption agent. α-Amylase was desorbed from the p(HEMA-MAT)-Ni^{2+} nanospheres at about 90% in this desorption medium.

Reusability of a matrix is an important necessity for large-scale applications. Thus, the adsorption–desorption cycle was repeated 5 times using the same nanospheres. As seen in Figure 8, no remarkable reduction in the adsorption capacity of the p(HEMA-MAT)-Ni^{2+} nanospheres was observed. As a result, p(HEMA-MAT)-Ni^{2+} nanospheres can be regarded as a reusable and economic adsorbent for enzyme immobilization.

2.7. Steady state kinetics

Enzymatic efficiency is affected by environmental parameters such as temperature and pH either in free or in immobilized forms. For this reason, activity studies were performed at various temperatures, pH levels, and substrate concentrations to determine the optimum conditions.

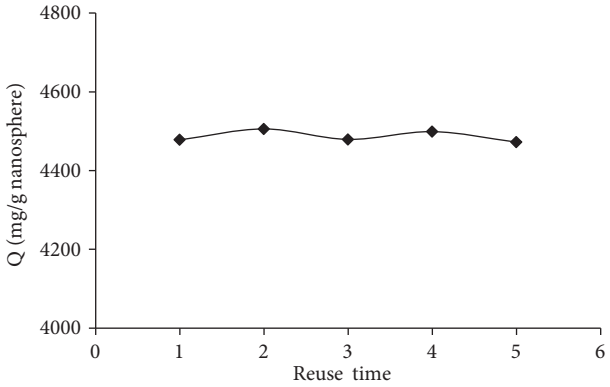

Figure 8. Reusability of the p(HEMA-MAT)-Ni^{2+} nanospheres (pH: 4.0; c: 1.0 mg/mL; time: 60 min, T: 25 °C).

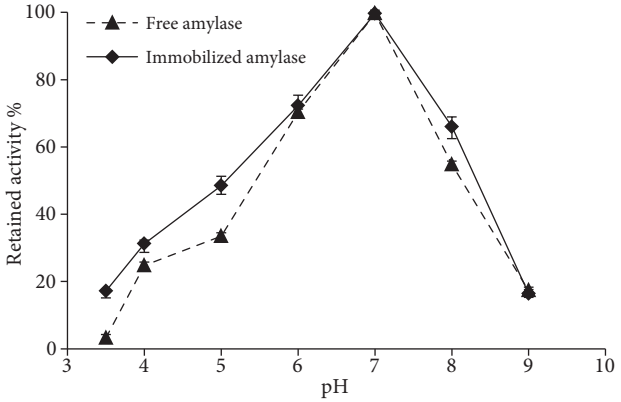

Figure 9. pH profiles of free and immobilized α-amylase (c: 1 mg/mL; T: 25 °C).

The proximate microenvironment of the enzyme molecule may affect its behavior. The optimum pH value of an enzyme in solution can be changed by immobilization on a solid matrix. The pH value in the immediate environs of the enzyme molecule may change due to the surface and residual charges on the solid matrix and the nature of the enzyme bound. Therefore, a shift can be observed in the pH optimum of the enzyme activity.[34] To determine the optimal pH values, adsorption of α-amylase (1 mg/mL) onto the p(HEMA-MAT)-Ni^{2+} nanospheres was studied in the pH range 3.5–9.0 at 25 °C. As seen in Figure 9, immobilized enzyme has the same pH optimum as the free enzyme (pH $\sim$7), and so immobilization did not change the optimal pH of α-amylase. The other remarkable observation with this pH study was that the pH profile of the immobilized enzyme was broader than that of the free enzyme. This indicates that immobilization of the enzyme onto the p(HEMA-MAT)-Ni^{2+} nanospheres protects the enzyme activity in a wider pH range. Similar observations have been reported for immobilization of α-amylase and other enzymes.[11,35] Diffusional limitations or secondary interactions between the enzyme and the carrier may also influence this change.[36] Consequently, sensitivity to pH can be reduced as a result of immobilization.

To determine the optimum temperature, the enzyme activity was assayed in the temperature range 5–45 °C. Figure 10 shows the change in temperature profile with immobilization. The maximum catalytic activity was achieved at 25 °C for both free and immobilized α-amylase. The alteration observed in the activity with changing temperature was as expected: increased activity was observed with increasing temperature up to the optimum reaction temperature and then the deactivation of the enzyme occurred in a reversible and/or irreversible way. Consequently, the activity increased to a peak and then fell. As seen in Figure 11, the thermostability of the immobilized enzyme is better than that of the free one. It can be concluded that the enzyme should be extensively utilized in the immobilized form. It was demonstrated by the authors that enzymes showed better thermostability because of attaching to a complementary surface of a rigid support in a multipoint.[37]

A Lineweaver–Burk plot was used to analyze catalytic properties of the free and immobilized enzymes. The Michaelis–Menten constant, K_M, and maximum activity, Vmax, of the free and immobilized enzymes were estimated at pH 7.0 and 25 °C. K_M values were calculated as 2.79 $\pm$ 0.09 and 3.02 $\pm$ 0.15 mg/mL for free and immobilized enzymes, respectively. Effective characteristics of the enzyme are reflected by K_M, depending upon both partitioning and diffusional effects. Generally, the K_M value is affected by diffusional

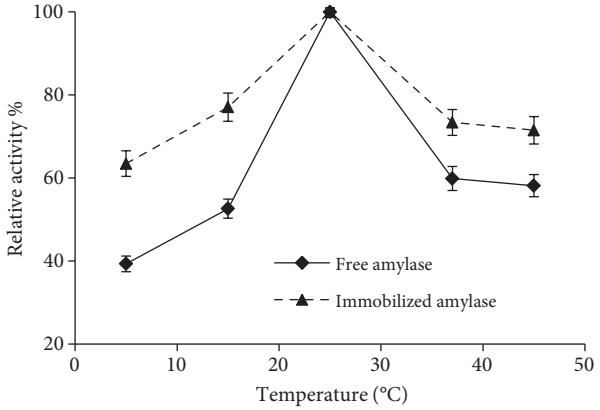

Figure 10. Temperature profiles of free and immobilized α-amylase (c: 1 mg/mL; pH: 7.0).

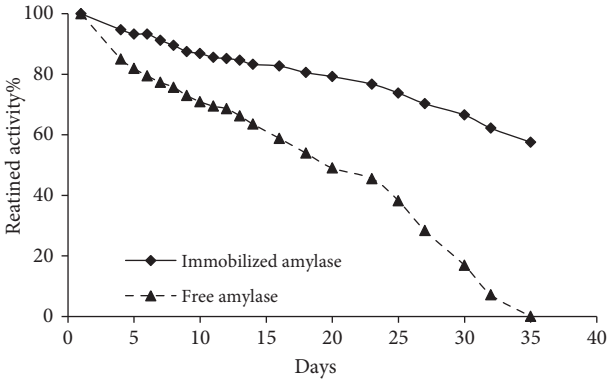

Figure 11. Storage stability of free and immobilized α-amylase (pH: 7.0, c: 1 mg/mL; T: 4 °C).

limitations, steric effects, and ionic strength. Thus, an immobilized enzyme has higher K_M than does the free enzyme.[38] Structural changes in the enzyme by the immobilization procedure cause alteration in the affinity of the enzyme for its substrate and lower accessibility of the substrates to the active site of the immobilized enzyme.[39] The results showed that the affinity of α-amylase to its substrate was not significantly changed by immobilization. Vmax is an intrinsic characteristic of the immobilized enzyme, because it specifies the highest possible velocity when the entire enzyme is saturated with substrate. However, diffusional restraints may also affect Vmax.[40] Vmax values for the free and immobilized enzymes were 13.05 $\pm$ 0.53 U/mg and 12.92 $\pm$ 0.41 U/mg, respectively. No significant change in this kinetic parameter was observed upon immobilization.

2.8. Storage stability

Enzymes are susceptible to environmental conditions and are not stable in solutions; thus they may lose their activities quite easily.[41,42] To improve the storage stability of an enzyme by immobilization can be an impressive advantage for preparative or industrial usage. For this reason, storage stability experiments using free and immobilized α-amylase preparations were carried out for a period of 5 weeks with storage conditions of phosphate buffer (50 mM; pH 7.0) and 4 °C. Both free and the immobilized enzyme preserved their initial activities during the first 5 days. All the activity of the free enzyme was lost within 35 days, whereas 42.4% of activity of the immobilized enzyme was lost during roughly the same period (Figure 11). According to our results, it can be concluded that the reason for the decrease in activity can be a time-dependent natural loss in enzyme activity and this decrease can be prevented to a significant degree by immobilization. Various researchers have also reported improved storage stability with immobilization.[43,44]

3. Experimental

3.1. Materials

HEMA (Sigma Chem., St. Louis, MO, USA) and ethyleneglycoldimethacrylate (EGDMA, Aldrich, Munich, Germany) were distilled under vacuum (100 mmHg). *Aspergillus oryzae* α-amylase, starch, and 3,5-dinitrosalicylic acid were all obtained from Sigma (St. Louis, MO, USA). All other chemicals were of the highest purity commercially available and were used without further purification. Ultrapure water filtered by Millipore (Molsheim, France) was used for all experiments unless otherwise stated. Before use, the laboratory glassware was rinsed with water and dried in a dust-free environment.

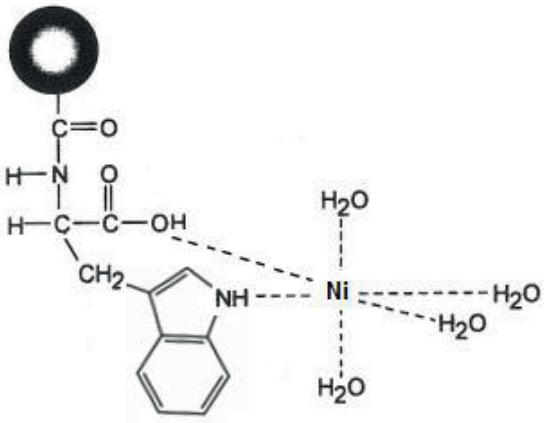

Figure 12. Schematic diagram for the chelation of Ni^{2+} ions through p(HEMA-MAT) nanospheres.

3.2. IMAC carrier for α-amylase immobilization

MAT was synthesized according to the method in the study by Akgol et al.[16] Average particle size of the p(HEMA-MAT) nanospheres produced by surfactant free emulsion polymerization is 100 nm with 1.158 particle size distribution (as polydispersity index (PDI)). The polymerization process can be summarized as follows. Polyvinyl alcohol (PVAL) used as stabilizer (0.5 g) was dissolved in 50 mL of deionized water. The comonomer mixture was added to the continuous phase prepared with PVAL. The dispersion was mixed in an ultrasonic bath for about 30 min. After the addition of the initiator, nitrogen gas flowed through the solution for about 1–2 min to remove dissolved oxygen. Polymerization was carried out in a constant temperature shaking bath at 70 °C under nitrogen atmosphere for 24 h. After the polymerization period, the polymeric nanospheres were centrifuged at 18,000 $\times$ g for 2 h (Zentrifugen, Universal 32 R, Germany). Washing was performed several times to remove the unreacted monomers and cross-linkers. The polymeric precipitate was resuspended in methanol and centrifuged again. Then the resuspension was prepared in deionized water and centrifuged again. $NiSO_4$ was used as Ni^{2+} ion source to prepare immobilized metal chelate affinity support. Equal volumes of 1000 mg/L Ni^{2+} solution and p(HEMA-MAT) nanospheres solution were mixed and stirred at 100 rpm for 24 h at room temperature. The unbound Ni^{2+} ions were removed by washing with ethanol and water. Ni^{2+} ion concentrations in the initial solution and at equilibrium were determined by atomic absorption spectrophotometer (PerkinElmer AA 700). The chelation between Ni^{2+} ions and p(HEMA-MAT) nanospheres can be demonstrated schematically in Figure 12.

In this study, Ni^{2+}-incorporated p(HEMA-MAT) nanospheres were used as a carrier for the immobilization of α-amylase.

3.3. Characterization of IMAC carrier

FTIR spectra of the nanospheres were obtained by FTIR spectrophotometer (PerkinElmer spectrum 100 FT-IR spectrometer) with a universal ATR sampling accessory. A Zeta Sizer (Malvern Instruments, Model 3000 HSA, UK) was used to determine particle size, size distribution, and surface charge. SEM analysis was performed to determine the surface morphology of the p(HEMA-MAT)-Ni^{2+} nanospheres. The samples were initially dried in air at 25 °C for 7 days before being analyzed. A part of the dried bead was mounted on a SEM sample mount and was sputter coated for 2 min. The sample was then mounted in a scanning electron microscope (SEM,

Phillips, XL-30S FEG, Germany). The surface of the sample was then scanned at the desired magnification to study the morphology of the nanospheres. The following expression was used to calculate the surface area of p(HEMA-MAT)-Ni^{2+}.

$$N = \frac{6 \times 10^{10} \times S}{\pi \times q_s \times d^3}, \tag{1}$$

where N is the number of nanospheres per milliliter, S is the solids %, q_s is the density of bulk polymer (g/mL), and d is the diameter (nm). The number of nanospheres in 1 mL of suspension was determined from the mass–volume graph of nanospheres. From all these data, the specific surface area of p(HEMA-MAT)-Ni^{2+} nanospheres was calculated by multiplying N and the surface area of 1 nanosphere.

An elemental analyzer (Leco, CHNS-932, USA) was used to determine the degree of MAT incorporation into the synthesized p(HEMA-MAT) nanospheres.

3.4. Adsorption studies with α-amylase

$\alpha-$Amylase adsorption on the p(HEMA-MAT)-Ni^{2+} nanospheres was performed in the medium of different pHs (3.5–9.0), α-amylase concentrations (0.25–1.25 mg/mL), temperatures (5–45 °C), and ionic strengths (0.0–1.0 M NaCl). α-Amylase adsorption studies were performed in a batch system for 1 h at 25 °C. The initial and final concentrations of α-amylase were determined by UV/Vis spectrophotometer (Shimadzu 1601, Japan). The amount of adsorbed α-amylase per unit mass of the on the p(HEMA-MAT)-Ni^{2+} nanospheres was calculated using the following expression:

$$Q = \frac{(C_0 - C) \times V}{m}, \tag{2}$$

where Q is the amount of α-amylase adsorbed onto unit mass of the nanospheres (mg/g), C_0 and C are the concentrations of α-amylase in the initial solution and in the supernatants obtained after centrifugation at 18,000 $\times g$, respectively (mg/g), V is the solution volume (mL), and m is the mass of the nanospheres used (g).

The adsorption experiments were performed in replicates of 3. For each set of data present, standard statistical methods were used to determine the mean values and standard deviations. Confidence intervals of 95% were calculated for each set of samples in order to determine the margin of error.

3.5. Desorption and repeated use

Desorption experiments on α-amylase were performed using different desorption agents. To obtain most efficient recovery yield 1.0–1.5 M NaCl and 1 M NaSCN were used. The α-amylase immobilized p(HEMA-MAT)-Ni^{2+} nanospheres were incubated in desorption medium at room temperature for 2 h. The desorption ratio was calculated from the amount of α-amylase adsorbed on the nanospheres and the final protein concentration in the desorption medium.

$$\text{Desorption ratio}(\%) = \frac{\text{Amount of } \alpha\text{-amylase desorbed}}{\text{Amount of } \alpha\text{-amylase adsorbed}}, \times 100 \tag{3}$$

In order to test the repeated use of p(HEMA-MAT)-Ni^{2+} nanospheres, the α-amylase adsorption–desorption cycle was repeated 5 times using the same nanospheres.

3.6. Activity assays of free and immobilized α-amylase

Activities of free and immobilized α-amylase were determined by the assay suggested by Bernfeld wherein the reducing groups liberated from starch are measured by the reduction of 3,5-dinitrosalicylic acid.[30]

The assay mixture includes 30% sodium-potassium tartarate (w/v), 1.6% NaOH (w/v), and 1% DNSA (w/v). Equal volumes of enzyme and starch solutions were mixed and incubated at room temperature for 3 min and then the assay mixture was added to the enzyme–substrate mixture as an equal volume of this mixture. This solution was incubated in boiling water for 5 min. After cooling, the solution was diluted with distilled water and the intensity of the red color that developed was measured in a UV/Vis spectrophotometer (Shimadzu, Model 1601) at 540 nm.

In each set of experiments, different concentrations of starch were used to prepare a standard curve. Nonreducing ends of starch were determined as described, and the results were converted to relative activities (percentage of the maximum activity obtained in the series). Hydrolytic activity evaluated after enzyme immobilization on the p(HEMA-MAT)-Ni^{2+} compared with activity of the same quantity of free enzyme and residual activity was determined. One unit liberates from soluble starch 1 μmol of reducing groups (calculated as maltose) per minute at 25 °C and pH 6.9 under the specified conditions.[30]

$$\text{Units/mg} = \frac{\text{Micromoles maltose liberated}}{\text{mg of enzyme in reaction mixture} \times 3\,\text{min}} \tag{4}$$

3.7. Steady state kinetics

Activity assays were carried out over the pH range of 3.5–9.0 and temperature range of 5–45 °C so as to determine pH and temperature profiles for the free and immobilized α-amylase. Activity results dependent on pH and temperature are presented in a standardized form with the highest value of each set being appropriated as the value of 100% activity.

The activity assay was performed with different starch concentrations to determine the effect of substrate concentration on both free and immobilized enzyme activities. The substrate concentrations varied from 0.1 to 1.0 g/L in 50 mM phosphate buffer at optimum pH. The Michaelis constant (K_M) and V_{max} were determined using a Lineweaver–Burk plot. All parameters were the mean of triplicate determinations from 3 independent preparations.

4. Conclusions

To stabilize enzymes with improved intrinsic and operational stabilities may be possible with the development of nanomaterials and nanostructured materials. Recently, studies have focused on the development of suitable low-cost sorbents. Ni^{2+}-chelated p(HEMA-MAT) nanospheres used for the immobilization of α-amylase in this study provide many advantages over conventional techniques. Coupling of a chelating ligand to the adsorption matrix is an expensive and critical step in the preparation process of metal-chelating sorbent. In this procedure, loading the metal ion directly on the nanospheres without further modification steps is possible, because comonomer MAT acts as the metal-chelating ligand. Slow release of these covalently bonded chelators from the sorbent is the other important point. A general problem encountered in any immobilized metal-chelate affinity adsorption technique is metal-chelating ligand release, which causes a decrease in adsorption capacity. MAT playing a role as metal-chelating ligand and/or comonomer was polymerized with HEMA and there was no leakage of the ligand. The difficulty of multistep purification methods will be solved by this purification method.

Low cost and resistance to harsh operation conditions and high temperature are desirable features of the p(HEMA-MAT)-Ni^{2+} nanospheres. p(HEMA-MAT)-Ni^{2+} nanospheres exhibited quite high binding capacity (4468.1 $\pm$ 177.5 mg/g) due to their highly specific surface. Immobilization did not drastically change the optimum pH or temperature profile of the immobilized enzyme, but the thermostability of immobilized α-amylase was better than that of the free one. The storage stability of the immobilized enzyme was also higher than that of the soluble enzyme under similar conditions. The reusability and the higher storage stability of immobilized α-amylase presented in this work may provide economic advantages for large-scale biotechnological applications.

References

1. Schenck, F. W.; Hebeda, R. E. *Starch Hydrolysis Products: Worldwide Technology, Production and Applications*, VCH, New York, 1992.
2. Windish, W. W.; Mhatre, N. S. *Advances in Applied Microbiology*, In: Wayne, W. U. Ed., 1965.
3. Fogarty, W. M.; Kelly, C. T. In *Topics in Enzyme and Fermentation Biotechnology*; Wiseman, A., Ed., 1979.
4. Vihinen, M.; Mantsala, P. *Crit Rev. Biochem. Mol. Biol.* **1989**, *24*, 329–418.
5. Lonsane, B. K.; Ramesh, M. V. *Adv. Appl. Microbiol.* **1990**, *35*, 1–56.
6. Nikolov, Z. L.; Reily, P. J. In *Biocatalysts for Industry*; Dordick, J. S., Ed. Plenum Press, New York, 1991.
7. Liu, Y.; Jia, S.; Ran, J.; Wu, S. *Catal. Commun.* **2010**, *11*, 364–367.
8. Yamamoto, T. In *Handbook of Amylases and Related Enzymes: Their Source, Isolation Methods, Properties and Applications*; Amylase Research Society of Japan, Ed., Pergamon Press, Oxford, 1988.
9. Bahar, T.; Celebi, S. S. *Enzyme Microb. Technol.* **2000**, *26*, 28–33.
10. Roig, M. G.; Kennedy, J. F.; Garaita, M. G. *J. Biomater. Sci. Polym. Ed.* **1994**, *6*, 661–673.
11. Ida, J.; Matsuyama, T.; Yamamoto, H. *Biochem. Eng. J.* **2000**, *5*, 179–184.
12. Yang, Y.; Chase, H. A. *Biotechnol. Appl. Biochem.* **1998**, *28*, 145–154.
13. Chen, J. P.; Sun, Y. M.; Chu, D. H. *Biotechnol. Prog.* **1998**, *14*, 473–478.
14. Bryjak, J. *Bioprocess Eng.* **1995**, *13*, 177–181.
15. Mateo, C.; Palomo, J. M.; Fernandez-Lorente, G.; Guisan, J. M.; Fernandez-Lafuente, R. *Enzyme Microb. Technol.* **2007**, *40*, 1451–1463.
16. Akgol, S.; Ozturk, N.; Denizli, A. *J. Appl. Polym. Sci.* **2010**, *115*, 1608–1615.
17. Cong, L.; Kaul, R.; Dissing, U.; Mattiasson, B. *J. Biotechnol.* **1995**, *42*, 75–84.
18. Tischer, W.; Kashe, V. *Biotechnology* **1999**, *17*, 326–335.
19. Ye, P.; Xu, Z. K.; Che, A. F.; Wu, J.; Seta, F. *Biomaterials* **2005**, *26*, 6394–6403.
20. Rebros, V.; Rosenberg, M.; Mlichova, Z.; Kristofikova, L. *Food Chem.* **2007**, *102*, 784–787.
21. Sankalia, V.; Mashru, V.; Sankalia, J. M.; Sutariya, V. B. *Eur. J. Pharm. Biopharm.* **2007**, *65*, 215–232.
22. Peng, K.; Hidajat, K.; Udin, M. S. *J. Colloid Interface Sci.* **2004**, *271*, 277–283.
23. Choi, S. W.; Kwon, H. Y.; Kim, W. S.; Kim, J. H. *Colloids Surf. A* **2002**, *201*, 283–289.
24. Ozturk, N.; Akgol, S.; Arisoy, M.; Denizli, A. *Sep. Purif. Technol.* **2007**, *58*, 83–90.
25. Kim, J.; Grate, J. W.; Wang, P. *Chem. Eng. Sci.* **2006**, *61*, 1017–1026.
26. Tuzmen, N.; Kalburcu T.; Denizli A. *Process Biochem.* **2012**, *47*, 26–33.
27. Porath, J.; Carlson, J.; Olsson, I.; Belfrage, G. *Nature* **1975**, *258*, 598–599.

28. Gaberc-Porekar, V.; Menart, V. *J. Biochem. Biophys. Methods* **2001**, *49*, 335–360.
29. Arnold, F. H. *Bio. Technology* **1991**, *9*, 150–155.
30. Gutierrez, R. E.; Martin del Vale, M.; Galan, M. A. *Sep. Purif. Rev.* **2007**, *36*, 71–111.
31. Kubota, N.; Nakagawa, Y.; Eguchi, Y. *J. Appl. Polym. Sci.* **1996**, *62*, 1153–1160.
32. Lawal, O. S. *Food Chem.* **2006**, *95*, 101–107.
33. Ueda, E. K. M.; Gout, P. W.; Morganti, L. *J. Chromatogr. A* **2003**, *988*, 1–23.
34. Mosbach, K. *Sci. Am.* **1971**, *224*, 26–33.
35. He, D.; Cai, Y.; Wei, W.; Nie, L.; Yao, S. *Biochem. Engineer. J.* **2000**, *6*, 7–11.
36. Tanyolac, D.; Yuruksoy, B. I.; Ozdural, A. R. *Biochem. Eng. J.* **1998**, *2*, 179–186.
37. O'Neill, S. P.; Dunnill, P.; Lilly, M. D. *Biotechnol. Bioeng.* **1971**, *13*, 337–352.
38. Lopez, G. P.; Ratner, B. D.; Rapoza, R. J.; Horbett, T. A. *Macromol. Symp.* **1993**, *26*, 3247–3253.
39. Arica, M. Y.; Senel, S.; Alaeddinoglu, N. G.; Patir, S.; Denizli, A. *J. Appl. Polym. Sci.* **2000**, *75*, 1685–1692.
40. Aksoy, S.; Tumturk, H.; Hasirci, N. *J. Biotechnol.* **1998**, *60*, 37–46.
41. Turunc, O.; Kahraman, M. V.; Akdemir, Z. S.; Kayaman-Apohan, N.; Güngör, A. *Food Chem.* **2009**, *112*, 992–997.
42. Kara, A.; Osman, B.; Yavuz, H.; Beşirli N., Denizli A. *React. Funct. Polym.* **2005,** *62*, 61–68.
43. Chang, M. Y.; Juang, R. S. *Process Biochem.* **2004**, *39*, 1087–1090.
44. Reddy, K. R. C.; Kayastha, A. M. *J. Mol. Catal. B: Enzym.* **1994**, *38*, 104–112.